Modeling and Kinetic Analysis of the Reaction System Using Whole Cells with Separately and Co-Expressed D-Hydantoinase and *N*-Carbamoylase

Joo-Ho Park,[*] Ki-Hoon Oh, Dong-Cheol Lee,[†] Hak-Sung Kim

Department of Biological Sciences, Korea Advanced Institute of Science and Technology, 373-1, Kusung-dong Yusung-gu, Taejon, 305-701, Korea; telephone: 82-42-869-2616; fax: 82-42-869-2610; e-mail: hskim@mail.kaist.ac.kr

Received 30 August 2001; accepted 7 January 2002

DOI: 10.1002/bit.10259

Abstract: We developed a kinetic model that describes a heterogeneous reaction system for the production of D-*p*-hydroxyphenylglycine from D,L-*p*-hydroxyphenylhydantoin using D-hydantoinase of *Bacillus stearothermophilus* SD1 and *N*-carbamoylase of *Agrobacterium tumefaciens* NRRL B11291. As a biocatalyst, whole cells with separately or co-expressed enzymes were used. The reaction system involves dissolution of substrate particles, enzymatic conversion, racemization of the L-form substrate, and transfer of the dissolved substrate, intermediate, and product through the cell membrane. Because the two enzymes have different pH optimum, kinetic parameters were evaluated at different pH for the reaction systems. The model was simulated using the kinetic parameters and compared with experimental data, and it was found that the kinetic model well describes the behavior of the reaction systems using whole cells with separately and co-expressed enzymes. Factors affecting the kinetics of the reaction systems were analyzed on the basis of the kinetic model. In the reaction system with separately expressed enzymes, racemization rate and transport of the reaction intermediate (*N*-carbamoyl-D-*p*-hydroxyphenylglycine) were revealed to be the limiting factors at neutral pH, resulting in accumulation of intermediate in the reaction medium. At alkaline condition, on the other hand, inhibition of *N*-carbamoylase by ammonia was severe, and thereby the reaction rate significantly reduced. In the co-expressed enzyme system, accumulation of intermediate was negligible in the reaction medium, and the improved performance was observed compared to that with separately expressed enzymes. The present model might be applied for the optimization and development of the reaction system using two sequential enzymes. *Biotechnol Bioeng* **78**: 779–793, 2002.

Keywords: D-hydantoinase; *N*-carbamoylase, D-amino acids; kinetic model; simulation

Correspondence to: H. S. Kim

*Present address: R & D Center of Pharmaceuticals/Cheil Jedang Corp., 522-1, Dokpyong-ri, Majang-myon, Ichonsi, Kyonggi-do, 467-810, Korea

†*Present address:* Department of Bio & Information, Chungbuk Provincial University of Science and Technology, 40, Kumgu4-ri, Okcheon-go, Chungbuk, 373-807, Korea

INTRODUCTION

Optically active D-amino acids are widely used as intermediates for the synthesis of semi-synthetic antibiotics, peptide hormones, pyrethroids, and pesticides. In the D-hydantoinase-catalyzed process developed by Yamada et al. (1978), the chemically synthesized D,L-5-mono-substituted hydantoin is enantioselectively hydrolyzed to the corresponding *N*-carbamoyl-D-amino acid by D-hydantoinase, and this intermediate is further converted to free D-amino acid by *N*-carbamoyl-D-amino acid amidohydrolase (*N*-carbamoylase) or chemical decarbamoylation (Fig. 1). There have been a number of studies regarding isolation and characterization of hydantoinases (Keil et al., 1995; Lee et al., 1995; Sudge et al., 1998; Syldatk et al., 1999), mass production of enzymes (Abendroth et al., 2000; Lee et al., 1997), and process development (Chao et al., 1999; Lee and Kim, 1998). We recently reported modeling and kinetic analysis of the heterogeneous reaction system using mass-produced D-hydantoinase for optimization of chemo-enzymatic process (Lee et al., 1999). Chemical decarbamoylation, however, has a couple of drawbacks such as low yield and large disposal of waste, and much attention has been paid to development of a fully enzymatic process employing D-hydantoinase and *N*-carbamoylase.

Olivieri et al. (1981) reported the D-amino acid production using *Agrobacterium radiobacter* (*tumefaciens* to date) NRRL B11291 possessing both D-hydantoinase and *N*-carbamoylase. Recently, D-hydantoinase and *N*-carbamoylase of *Agrobacterium tumefaciens* were cloned into *Escherichia coli* and used as a biocatalyst for the D-amino acid production (Chao et al., 1999; Grifantini et al., 1998; Ogawa et al., 1994). We previously attempted a development of a fully enzymatic process employing D-hydantoinase from *Bacillus stearothermophilus* SD1 and *N*-carbamoylase of *A. tumefaciens* NRRL B11291 (Park et al., 2000). We used whole cells of *E. coli*

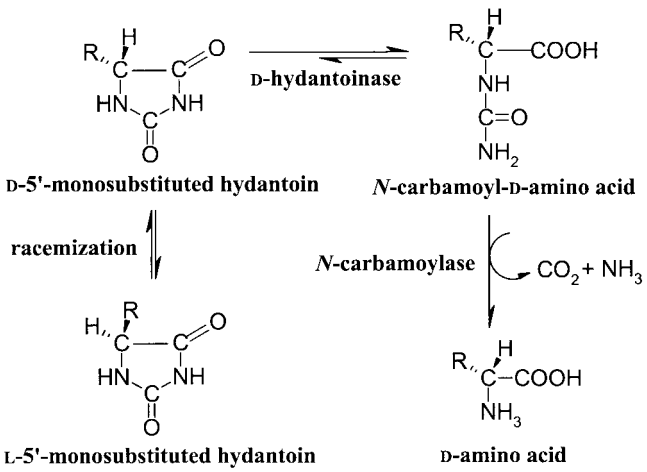

Figure 1. Reaction scheme for the production of D-amino acids from 5-monosubstituted hydantoins by D-hydantoinase and *N*-carbamoylase. *R* indicates the functional group.

with separately and co-expressed enzymes as a biocatalyst and compared two reaction systems quantitatively in terms of the reaction rate and product yield. Although a few cases using the two enzymes were reported (Chao et al., 1999, Park et al., 2000), the detailed kinetic analysis of the reaction system using D-hydantoinase and *N*-carbamoylase remains to be performed. Moreover, because the two enzymes have different optimal conditions and stability, kinetic analysis of the reaction system at various reaction conditions are prerequisite for optimization and development of the process.

In this work, we established the kinetic model, which describes the reaction system for the production of D-hydroxyphenylglycine from poorly soluble *p*-hydroxyphenylhydantoin using whole cells with separately and co-expressed D-hydantoinase and *N*-carbamoylase. D-Hydantoinase of *B. stearothermophilus* SD1 and *N*-carbamoyl-D-amino acid amidohydrolase (*N*-carbamoylase) of *A. tumefaciens* NRRL B11291 were used as enzyme sources. No activity of *N*-carbamoylase was found in *B. stearothermophilus* SD1, and *N*-carbamoylase of *A. tumefaciens* NRRL B11291 was used as a second-step enzyme. The model involves dissolution of substrate particles, enzymatic conversion, racemization of the L-form substrate, and transfer of the dissolved substrate and product as well as intermediate across the cell membrane for the separately and co-expressed enzyme systems. Simulation of kinetic model was performed using the kinetic parameters and compared with the experimental results. Factors affecting the kinetics of the reaction system were also analyzed on the basis of the kinetic model.

MODEL DEVELOPMENT

To develop a kinetic model that describes the heterogeneous reaction system using D-hydantoinase and *N*-carbamoylase, the reaction system was analyzed in more detail. We previously reported the two different reaction systems using D-hydantoinase and *N*-carbamoylase. One is to use the whole cells with separately expressed enzymes and the other is the co-expressed enzyme system (Park et al., 2000). Figure 2 shows the schematic diagram of the two reaction systems. In both cases, the solid substrate, *p*-hydroxyphenylhydantoin (*p*-HPH), dissolves into the reaction mixture, and is transferred to inside cells. Only D-*p*-HPH inside cells is hydrolyzed to *N*-carbamoyl-D-hydroxyphenylglycine (NC-D-HPG) by D-hydantoinase, and L-*p*-HPH is spontaneously racemized to D-*p*-HPH as the reaction proceeds. In case of separately expressed enzyme system, the reaction intermediate, NC-D-HPG, diffuses out into the reaction medium from the D-hydantoinase-expressing cells, and then is transferred into the *N*-carbamoylase-expressing cells. As for the co-expressed enzyme system, on the other hand, NC-D-HPG is hydrolyzed to D-HPG by *N*-carbamoylase inside the same cells.

On the basis of the above analysis, we established a mathematical model for the reaction systems using whole cells with separately and co-expressed D-hydantoinase and *N*-carbamoylase.

Reaction System Using Whole Cells with Separately Expressed Enzymes

A schematic diagram for the reaction system using whole cells with separately expressed D-hydantoinase or *N*-carbamoylase is shown in Figure 2A. The starting substrate, *p*-HPH, is transferred into the cells and hydrolyzed to intermediate, NC-D-HPG, by D-hydantoinase. Produced NC-D-HPG is diffused out into the aqueous reaction medium through cell membrane. The intermediate is transferred into the cells expressing the *N*-carbamoylase and converted to D-HPG by the action of *N*-carbamoylase. The final product is diffused out to the reaction medium. Based on these considerations, we established the model that describes the reaction system using separately expressed enzymes as below.

The dissolution rate of solid substrate can be expressed as follows:

$$\frac{dS}{dt} = k_s a_p (S^* - S) \tag{1}$$

The dissolution process is independent of the substrate chirality, and the k_s is assumed to be constant over the range of reaction conditions. The size and shape of the substrate particles are presumed to be even and spherical.

The change of particle radius due to dissolution is given by

$$\frac{dR}{dt} = -\frac{k_s}{\rho_s}(S^* - S_{Da} - S_{La}) \tag{2}$$

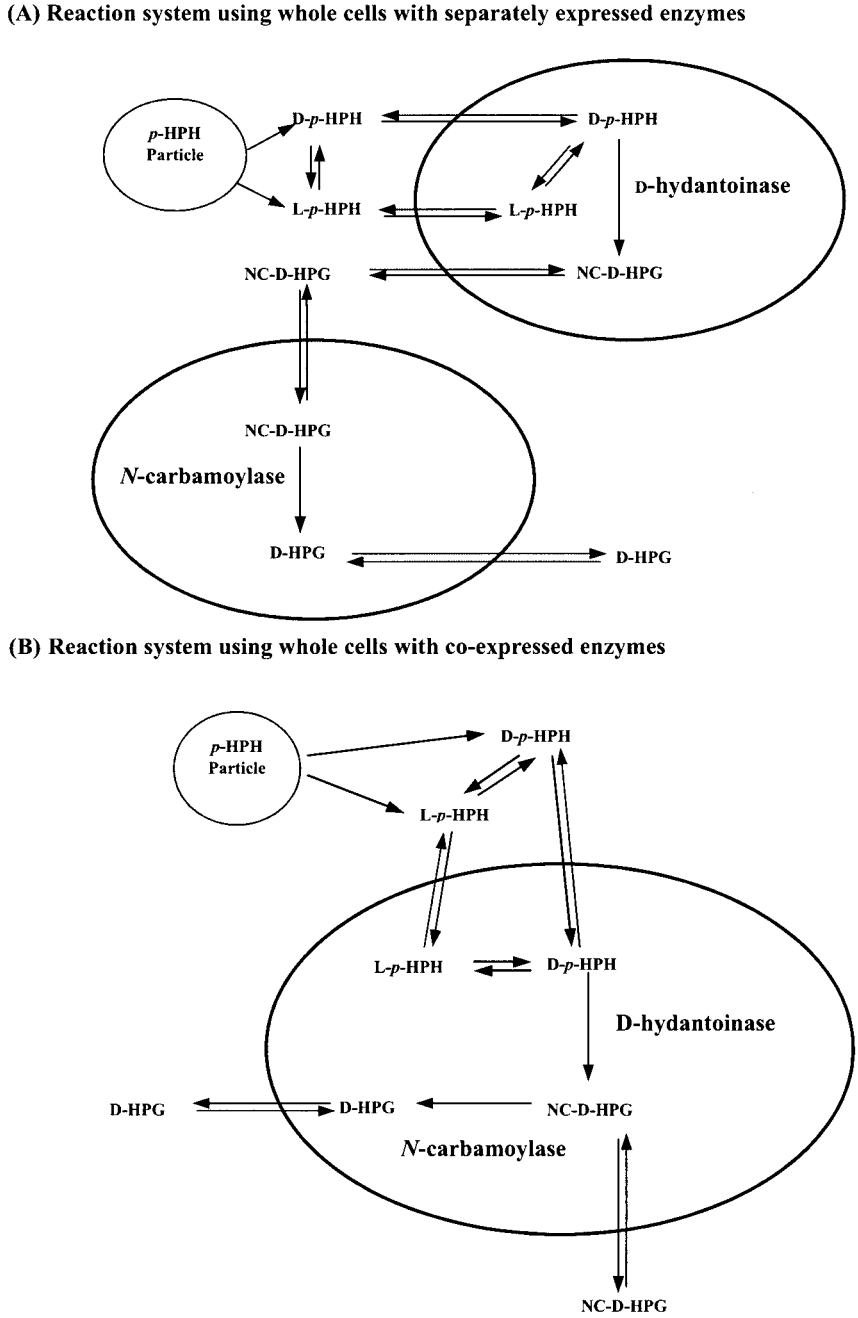

Figure 2. Schematic diagrams of the heterogeneous reaction systems using whole cells with separately expressed (A) and co-expressed (B) D-hydantoinase and *N*-carbamoylase.

As the concentration of D-form substrate decreases due to the enzyme reaction, the spontaneous racemization of L-form substrate to D-form occurs. The racemization rate is described by the first-order reversible reaction as

$$\frac{dS_D}{dt} = -\frac{dS_L}{dt} = k_R(S_D - S_L) \tag{3}$$

The variation in the concentrations of D-*p*-HPH and L-*p*-HPH in the aqueous solution depends on the dissolution rate of substrate particles, spontaneous racemization rates of two enantiomers, and transfer rate of substrate through cell membrane. The flux of substrate, intermediate, and final product from the aqueous solution into the cells across the membrane is assumed to follow Fick's first law of diffusion (Markus et al., 1999). From the mass balance, variations of D- and L-form substrates in the aqueous solution are expressed by

$$\frac{dS_{Da}}{dt} = k_s N_P 2\pi R^2 (S^* - S_{Da} - S_{La}) + k_R(S_{La} - S_{Da}) - \frac{h_S A_{hyd}(S_{Da} - S_{Di})}{V_a} \tag{4a}$$

$$\frac{dS_{La}}{dt} = k_s N_P 2\pi R^2 (S^* - S_{Da} - S_{La}) + k_R (S_{Da} - S_{La}) - \frac{h_S A_{hyd}(S_{La} - S_{Li})}{V_a} \quad (4b)$$

The permeability of each compound is assumed to vary according to the following equation as described in our previous work (Lee et al., 1999):

$$h = h_0 + (h_{\max} - h_0)\frac{t}{P_m + t} \quad (5)$$

Of the two isomers, dissolved D-form substrate is hydrolyzed to NC-D-HPG by D-hydantoinase within the cells, and the reaction rate is expressed by the simple Michaelis-Menten kinetics as

$$-\frac{dS_{Di}}{dt} = \frac{k_{ch} E_{hyd} S_{Di}}{k_{mh} + S_{Di}} \quad (6)$$

As for the deactivation of D-hydantoinase, there are several factors that cause the deactivation. We previously established a model based on the hypothesis that the free enzyme loses its activity by spontaneous deactivation, by the presence of solid substrate particles, and by titrant used for titration (Lee et al., 1999). In this work, deactivation of enzyme by titrant and substrate particles was assumed to be negligible in the case of whole cell enzyme reaction due to cell membrane. Thus, the enzyme loses its activity mainly through spontaneous deactivation, following the first-order kinetics as

$$-\frac{dE_{hyd}}{dt} = k_{dh} E_{hyd} \quad (7)$$

Change in the concentration of *p*-HPH inside the cells is affected by the transfer rate of dissolved *p*-HPH into the cells, spontaneous racemization rate of *p*-HPH, and consumption rate of D-*p*-HPH by D-hydantoinase. Of the two isomers, only dissolved D-*p*-HPH is hydrolyzed to NC-D-HPG by D-hydantoinase. The variations of D- and L-*p*-HPH inside the cells can be expressed as

$$\frac{dS_{Di}}{dt} = \frac{h_S A_{hyd}(S_{Da} - S_{Di})}{V_{hyd}} + k_R (S_{Li} - S_{Di}) - \frac{k_{ch} E_{hyd} S_{Di}}{k_{mh} + S_{Di}} \quad (8a)$$

$$\frac{dS_{Li}}{dt} = \frac{h_S A_{hyd}(S_{La} - S_{Li})}{V_{hyd}} + k_R (S_{Di} - S_{Li}) \quad (8b)$$

The intermediate produced by D-hydantoinase within the cells diffuses out to the aqueous solution, and then is transferred into the *N*-carbamoylase-expressing cells. Thus, the concentration of intermediate inside the D-hydantoinase-expressing cells is given by

$$\frac{dM_{ih}}{dt} = \frac{k_{ch} E_{hyd} S_{Di}}{k_{mh} + S_{Di}} - \frac{h_M A_{hyd}(M_{ih} - M_a)}{V_{hyd}} \quad (9)$$

The intermediate concentration in the aqueous solution is influenced by the transfer rate of intermediate from the inside of the D-hydantoinase-expressing cells to the aqueous solution, and the transfer rate of intermediate from the aqueous solution into the *N*-carbamoylase-expressing cells. Mass balance for the intermediate yields the change of intermediate concentration in the aqueous solution as

$$\frac{dM_a}{dt} = \frac{h_M A_{hyd}(M_{ih} - M_a)}{V_a} - \frac{h_M A_{car}(M_a - M_{ic})}{V_{car}} \quad (10)$$

It has been known that *N*-carbamoylase is seriously inhibited by ammonia at alkaline condition (Olivieri et al., 1981; Runser et al., 1990). Inhibition study also revealed that the enzyme is inhibited by ammonia in a non-competitive pattern (Fig. 4). Based on these observations, we established the reaction kinetics of *N*-carbamoylase as

$$-\frac{dM_{ic}}{dt} = \frac{k_{cc} E_{car}}{\left(1 + \frac{I_{ic}}{k_i}\right)} \frac{M_{ic}}{M_{ic} + k_{mc}} \quad (11)$$

It was assumed that deactivation of *N*-carbamoylase within the cells follows the first-order kinetics as

$$-\frac{dE_{car}}{dt} = k_{dc} E_{car} \quad (12)$$

The concentration of NC-D-HPG inside the *N*-carbamoylase-expressing cells varies with the transfer rate of intermediate from the aqueous solution and consumption rate of intermediate by *N*-carbamoylase. Thus, the variation of NC-D-HPG inside the cells is given by

$$\frac{dM_{ic}}{dt} = \frac{h_M A_{car}(M_a - M_{ic})}{V_{car}} - \frac{k_{cc} E_{car}}{\left(1 + \frac{I_{ic}}{k_i}\right)} \frac{M_{ic}}{M_{ic} + k_{mc}} \quad (13)$$

The final product is formed by the *N*-carbamoylase within the cells, and production rate of the final product is affected by the enzyme reaction rate and the transfer rate of D-HPG to the aqueous solution. From the mass balance, the change in the final product concentration within the cells can be expressed as

$$\frac{dP_{ic}}{dt} = \frac{k_{cc} E_{car}}{\left(1 + \frac{I_{ic}}{k_i}\right)} \frac{M_{ic}}{M_{ic} + k_{mc}} - \frac{h_P A_{car}(P_{ic} - P_a)}{V_{car}} \quad (14)$$

Variation of the final product in the aqueous solution is simply derived from the concentration difference between the aqueous phase and inside cells as

$$\frac{dP_a}{dt} = \frac{h_P A_{car}(P_{ic} - P_a)}{V_a} \quad (15)$$

Reaction System using Whole cells with Co-expressed Enzymes

The reaction system using whole cells with co-expressed enzymes is schematically shown in Figure 2B. In this case, conversion of starting substrate to the final product occurs inside the same cells, and transport of intermediate is omitted from the kinetic model for the separately expressed enzymes system. It was assumed that whole cells with co-expressed enzymes have the same surface area and volume as those with separately expressed enzymes. Detailed description of the co-expressed enzyme system is given below.

The changes of substrate concentration in the aqueous solution and within the cells are the same as the separately expressed enzyme system. Moreover, substrate dissolution rate, reduction rate in substrate particle size, and permeability change are supposed to be identical to the reaction system using separately expressed enzymes.

Concentration of the intermediate inside the cells is dependent on both production rate of the intermediate by D-hydantoinase and consumption rate of the intermediate by *N*-carbamoylase. Diffusion rate of the intermediate to the reaction medium also affects the intermediate concentration within the cells. From the mass balance, change in the intermediate concentration within the cells is given by

$$\frac{dM_i}{dt} = \frac{k_{ch}E_{hyd}S_{Di}}{k_{ch}+S_{Di}} - \frac{k_{cc}E_{car}}{\left(1+\frac{I_i}{k_i}\right)}\frac{M_i}{M_i+k_{mc}} - \frac{h_M A_{Co}(M_i-M_a)}{V_{co}} \tag{16}$$

Variation of the intermediate concentration in the aqueous solution is simply expressed in terms of the transfer rate of the intermediate from inside the cells to the aqueous solution as

$$\frac{dM_a}{dt} = \frac{h_M A_{co}(M_i-M_a)}{V_a} \tag{17}$$

The level of final product within the cells is influenced by the production rate from intermediate by *N*-carbamoylase and transfer rate of D-HPG to the aqueous solution. Thus, variation of the final product, D-HPG, within the cells is expressed as

$$\frac{dP_i}{dt} = \frac{k_{cc}E_{car}}{\left(1+\frac{I_i}{k_i}\right)}\frac{M_i}{M_i+k_{mc}} - \frac{h_P A_{co}(P_i-P_a)}{V_{co}} \tag{18}$$

The concentration of D-HPG in the aqueous solution is simply dependent on the transfer rate of D-HPG from inside the cells to the aqueous solution. The variation of D-HPG is thus given by

$$\frac{dP_a}{dt} = \frac{h_P A_{co}(P_i-P_a)}{V_a} \tag{19}$$

For the estimation of surface area and volume of cells, the shape of *E. coli* cells was assumed to be a round-ended rod with a dimension of 1.0 μm × 5.0 μm (Singleton and Sainsbury, 1987). Consequently, the volume and surface area of single cell were calculated to be about 3.7×10^{-18} m^3 and 1.6×10^{-11} m^2, respectively. Microscopic observations revealed that the integrity of the cells was maintained during the reaction, and the total number of cells was presumed to remain constant.

MATERIALS AND METHODS

Chemicals and Strains

D,L-*p*-Hydroxyphenylhydantoin (D,L-*p*-HPH) was purchased from Tokyo Kasei Kogyo Co. (Chuo-Ku, Tokyo). *N*-carbamoyl-D-hydroxyphenylglycine (NC-D-HPG) was obtained from D,L-*p*-HPH by using D-hydantoinase as described in our previous work (Lee et al., 1998). D-*p*-hydroxyphenylglycine (D-HPG) and all other chemicals were of analytical grade and purchased from Sigma (St. Louis, MO). *E. coli* XL1 Blue/pHU183 expressing D-hydantoinase, the *N*-carbamoylase expressing *E. coli* XL1 Blue/pBCAR 21, and *E. coli* XL1 Blue/pHCAR101 co-expressing the D-hydantoinase and *N*-carbamoylase were constructed as described in our previous works (Lee et al., 1996; Park et al., 2000).

Preparation of Whole Cell Enzyme

Recombinant cells with separately or co-expressed enzymes were cultivated as described in our previous work (Park et al., 2000). Luria-Bertani (LB) medium containing 125 μg/mL of ampicillin was used for the production of D-hydantoinase and *N*-carbamoylase. Cells were cultivated in a 5-liter jar containing 3 liters of LB medium for 12 h. Temperature and initial pH were 30°C and 6.8, respectively. Cells were collected by centrifugation and washed twice with PBS (phosphate-buffered saline) solution containing 1 m*M* dithiothreital (DTT) and used for the whole cell enzyme reaction.

Enzyme Reaction

A stirred tank type reactor equipped with a propeller-type impeller was used for D-HPG production from D,L-*p*-HPH. The initial volume of the reaction mixture was 1 liter, and distilled water was used as the reaction medium. The predetermined amounts of whole cells were added to the reaction mixture containing 1 m*M* of $MnCl_2$ and DTT. When the whole cells with separately expressed D-hydantoinase and *N*-carbamoylase were used, the ratio of the activities between the two enzymes was controlled by changing the loading of individual cells. In the case of the reaction using whole cells ex-

pressing both two enzymes, collected cells were added to the reaction mixture after the specific activity of each enzyme was measured under standard assay conditions. The reaction was conducted at 45°C, and pH of the reaction mixture was controlled at the specified value with 1 N HCl and 1 N NaOH during the reaction. Nitrogen gas was sparged with a flow rate of 0.5 v/v/m for the prevention of substrate oxidation (Lee et al., 1998). At intervals, aliquots were taken and analyzed by using high-performance liquid chromatography (HPLC).

Determination of Racemization Constant

To determine the racemization rate of *p*-hydroxyphenylhydantoin at different pH values, we synthesized the optically pure D-*p*-HPH as following. Forty-five percent of NaCNO (25.43 g) was added drop-wise to a mixture of D-HPG (45 g) and water (45 mL) at 70°C for 6 h. After the distilled water (45 mL) was added to a reaction mixture, the reaction further continued for 4 h at 85°C, and then cooled at room temperature. The resulting white precipitate was filtered out and washed with water twice and dried at 70°C for 10 h. The purity of isolated *p*-HPH was determined by using HPLC.

The reaction mixture for the determination of racemization constant contained 5 m*M* D-*p*-HPH in the distilled water. The pH of the reaction medium was adjusted by using 0.1 *M* NaOH at 45°C, and reaction medium was agitated at 150 rpm for homogeneous mixing. At intervals, aliquots were taken, and the amounts of produced L-*p*-HPH and remaining D-*p*-HPH were analyzed using Chiral β-CD column (YMC Co., Japan). The mobile phase was 50 m*M* Na_3PO_4 (pH 4.1) and the flow rate was 0.8 mL/min. The column eluent was detected at 214 nm. The racemization rate constant was determined by fitting the experimental data into the kinetic equation of the first-order racemization reaction (see Eq. 3) at different pH values.

Determination of Inhibition Constant of Ammonia

The reaction mixture was composed of 1 m*M* of DTT, 5 μg of *N*-carbamoylase, and predetermined concentration of NH_4Cl in the 1 mL sodium phosphate buffer at specified pH value. After incubation at 45°C for 30 min, equal volume of 100 m*M* sodium phosphate buffer containing 5 g/L NC-D-HPG at the same pH was added to the reaction tube. The reaction mixture was incubated at 45°C, and the produced D-HPG was analyzed by using HPLC. Inhibition constant was determined by double-reciprocal plot of the initial reaction rate of *N*-carbamoylase as a function of substrate concentration in the presence and absence of NH_4Cl. The concentration of NH_4Cl used was in the range of 0 ~ 20 m*M*.

Analysis

The concentrations of D,L-*p*-HPH, NC-D-HPG, and D-HPG were determined using HPLC (Shimadzu, Japan). The column used was CLC-ODS (4.6 × 250 mm, Shimadzu, Japan). Ten percent (v/v) acetonitrile solution (pH 3.0) was used as the mobile phase, and the flow rate was 1.0 mL/min. The column eluent was detected at 214 nm. Biomass concentration was estimated by measuring the absorbance at 600 nm.

Parameter Evaluation

Kinetic parameters used in the equations were determined by various methods, and are summarized in Table I. The k_{cat} and k_m of D-hydantoinase and *N*-carbamoylase at different pH values were determined by double-reciprocal plot of experimental data as described in our previous work (Lee et al., 1999). First-order deactivation constants for D-hydantoinase and *N*-carbamoylase were determined by tracing the time course of the change in each enzyme activity at the specified conditions. The solubility of *p*-HPH was measured in the distilled water that had been adjusted to the prede-

Table I. Kinetic parameters used for the simulation of the reaction systems with separately expressed and co-expressed enzymes.

Parameter	Value	Dimension
R	0.03	cm
k_S	1.0×10^{-3}	cm/s
h_{max}	3.5×10^{-6}	cm/s
h_{S0}	3.5×10^{-8}	cm/s
P_m	2.0×10^{4}	s
k_R		
pH 7.0	2.1×10^{-4}	cm/s
pH 7.5	1.0×10^{-4}	
pH 8.0	3.2×10^{-5}	
k_{cat} (hydantoinase)		
pH 7.0	10.3	s^{-1}
pH 7.5	23.6	
pH 8.0	25.8	
k_m (hydantoinase)		
pH 7.0	6.29×10^{-2}	mole/L
pH 7.5	3.02×10^{-2}	
pH 8.0	1.03×10^{-2}	
k_d (hydantoinase)		
pH 7.0	4.02×10^{-6}	s^{-1}
pH 7.5	3.61×10^{-6}	
pH 8.0	3.11×10^{-6}	
k_{cat} (carbamoylase)		
pH 7.0	5.02	s^{-1}
pH 7.5	4.57	
pH 8.0	4.52	
k_m (carbamoylase)		
pH 7.0	1.02×10^{-3}	mole/L
pH 7.5	1.20×10^{-3}	
pH 8.0	1.86×10^{-3}	
k_d (carbamoylase)		
pH 7.0	4.91×10^{-5}	s^{-1}
pH 7.5	7.22×10^{-5}	
pH 8.0	8.18×10^{-5}	

termined pH at 45°C by using a spectrophotometer according to the procedure reported elsewhere (Constantinides, 1980), and the density of *p*-HPH was estimated by using the method described elsewhere (Shugar and Ballinger, 1996). The racemization rate constant of *L*-form substrate to *D*-form was determined by fitting the experimental data at different pH values as mentioned above.

The mass transfer coefficient of *p*-HPH, k_s, was estimated from a simple correlation with critical suspension speed and Schmidt number ($\mu/\rho D$) in the mechanically agitated tank as described elsewhere (Jadhav and Pangarkar, 1991). The permeability of each compound was estimated based on the data in the literature (Tranchino and Melle, 1990). Other parameters appeared in the kinetic model were estimated by using Marqurdt's method of non-linear regression analysis (Constantinides, 1980; Johnson and Faunt, 1992) within 95% confidence interval.

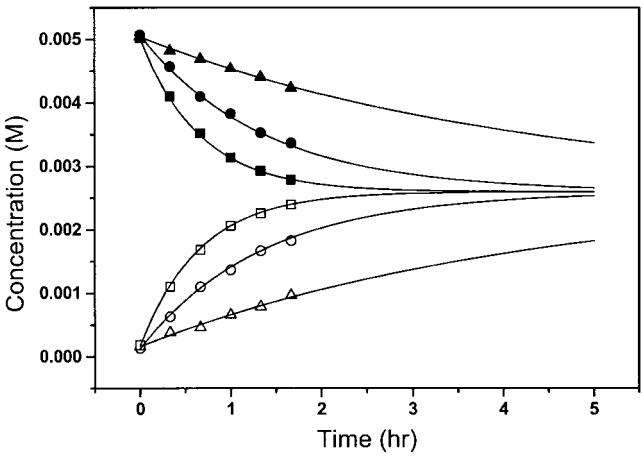

Figure 3. Spontaneous racemization of D-*p*-HPH at different pH values. Solid line and symbols represent the simulation results and experimental data, respectively. Closed and open symbols denote the D-*p*-HPH and L-*p*-HPH, respectively. Symbols are: D-*p*-HPH at pH 7.0 (▲), 7.5 (●), and 8.0 (■); L-*p*-HPH at pH 7.0 (△), 7.5 (○), and 8.0 (□).

Solution of Model Equations

The model equations for the whole cell reactions with separately and co-expressed enzymes were numerically integrated using the fourth-order Runge-Kutta method. The kinetic parameters shown in Table I were used for simulation. Non-linear regression analysis and integration of model equation were performed using the language of Borland C^{++}. An IBM PC with Pentium II microprocessor operating at 800 MHz was used in this work.

RESULTS AND DISCUSSION

Spontaneous Racemization Rate of L-Form Substrate

Keto-enol tautomerism is a typical feature of the hydantoin structure. Enolization between the 4- and 5-positions occurs under alkaline condition, which has been confirmed from the fact that optically pure hydantoin derivatives readily racemize spontaneously, even with both nitrogen atoms substituted. This racemization is of practical relevance for the complete conversion of racemic hydantoin derivatives to chiral α-amino acids. It has been reported, though, that racemization is accelerated by microbial enzyme racemase (Ishikawa et al., 1997; Wilms et al., 2001).

The rate of spontaneous racemization is known to be influenced by the electronic property of substituent at C-5. Substituents exerting an inductive effect with electronegativity stabilize the enolate structure because of the lowered electron density and consequently favored release of the proton at C-5. Therefore, hydantoins carrying a carboxyl function at an alkyl side chain will readily racemize. On the other hand, racemization of alkylated hydantoins might be very slow. Not only the property of substituent at C-5 of hydantoin but also pH condition influence the rate of racemization because the keto-form is dominant under neutral conditions. The racemization rate of hydantoins at neutral pH is much lower than at alkaline condition for these reasons.

Effect of pH on the racemization rate of *p*-HPH was evaluated at 45°C as described in the Materials and Methods section. Optically pure D-*p*-HPH was used as starting substrate, and produced L-*p*-HPH and remaining D-*p*-HPH were traced by using HPLC as shown in Figure 3. The racemization rate constant, k_R, was then determined by fitting the experimental data into the Equation 3 in the Model Development section. As a result, the rate constant for *p*-HPH at pH 8.0 was estimated to be 2.1×10^{-4} s^{-1}. As the pH lowered to 7.5 and pH 7.0, the rate constants decreased to 1.02×10^{-4} and 3.2×10^{-5} s^{-1}, respectively. The rate of racemization at pH 8.0 was one-order of magnitude higher than that at pH 7.0, which implies that the lower racemization rate of *p*-HPH at neutral pH might be a limiting factor in the overall reaction.

Development of a fully enzymatic process employing D-hydantoinase and *N*-carbamoylase would need the optimization of the reaction conditions because the two enzymes have different pH optimum as mentioned earlier: D-hydantoinase at pH 8.5, and *N*-carbamoylase at around pH 7.0. Thus, the enzyme reaction at neutral or acidic conditions might result in reduced racemization rate of substrate, leading to decrease in the production rate.

Inhibition of *N*-Carbamoylase by Ammonia

Olivieri et al. (1981) reported that *N*-carbamoylase is inhibited by ammonia, and that inhibition is more

serious at alkaline condition than at neutral or acidic pH. We determined the inhibition constant of ammonia at pH 7.0 and 8.0, respectively. As shown in Figure 4, the v_{max} of *N*-carbamoylase decreased when NH_4Cl was added to the reaction mixture, but k_m remained unchanged even in the presence of ammonium chloride. This result indicates that the *N*-carbamoylase is inhibited by ammonia in a non-competitive manner. Inhibition of *N*-carbamoylase by ammonia was found to be more serious at pH 8.0 than at neutral pH. Ammonium ion and carbon dioxide are simultaneously produced by the *N*-carbamoylase reaction. The produced ammonium ions are in equilibrium with ammonia, and their respective portion is dependent on the pH of reaction medium. The ammonium ions are dominant at neutral pH, but the concentration of ammonia at alkaline pH is 10 times higher than at neutral pH, which supports that *N*-carbamoylase is mainly inhibited by ammonia at alkaline condition.

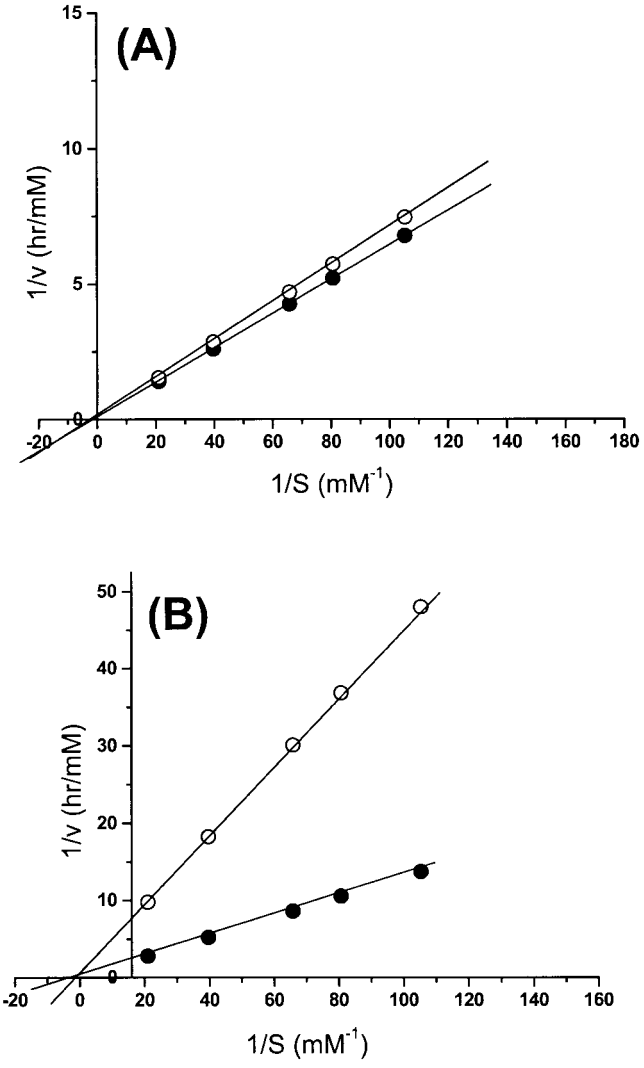

Figure 4. Inhibition of *N*-carbamoylase by ammonia at pH 7.0 (A) and pH 8.0 (B). The enzyme activity was determined at different substrate concentrations in the presence (○) or absence (●) of 20 m*M* NH_4Cl. *N*-Carbamoyl-D-*p*-hydroxyphenylglycin was used as substrate for *N*-carbamoylase.

The inhibition constants at pH 7.0 and 7.5 were determined to be 200 and 21 m*M*, respectively. However, inhibition constant at pH 8.0 was lowered to 8 m*M*, confirming the above results. At neutral pH, the inhibition was almost negligible compared to at alkaline pH. For the efficient production of D-amino acid at alkaline condition, the produced ammonia should be maintained at low level in the reaction mixture. We previously reported that deleterious effect of ammonia can be minimized by removing the produced ammonia using adsorbents in the free enzyme reaction (Kim and Kim, 1994).

Simulation of Reaction System with Separately Expressed Enzymes

The schematic reaction system using whole cells with separately expressed D-hydantoinase and *N*-carbamoylase is shown in Figure 2A. By using the kinetic parameters in Table I, production profiles were simulated at different pH values and compared with experimental data. The activities of D-hydantopinase and *N*-carbamoylase in the reaction medium were the same as 50 units per gram HPH.

As can be seen in Figure 5, the simulation results were well coincident with experimental data. At pH 7.0, the intermediate accumulated in the early phase of reaction and then reduced to almost zero as the reaction proceeded (Fig. 5A). The initial production rate of D-HPG was estimated to be about 8.75 m*M*/h, and the maximum concentration of intermediate reached 17.3 m*M*. The production of D-HPG almost linearly increased with time, which indicates that the intermediate available to the *N*-carbamoylase inside the cells was maintained at low level. This result seems to be attributable to different optimal conditions for two enzymes: D-hydantoinase exhibites a maximum activity at pH 8.5. On the other hand, the maximum activity of *N*-carbamoylase is observed at neutral pH. Thus, at pH 7.0, the production rate of NC-D-HPG by D-hydantoinase was low, and consequently transfer rate of NC-D-HPG into the *N*-carbamoylase-expressing cells reduced. However, the production profile at pH 7.5 was totally different from at pH 7.0 as shown in Fig. 5B. The intermediate accumulated at significant level, reaching up to 190 m*M* in 12 h, and the initial production rate of D-HPG decreased to 5.2 m*M*/h. No further increase in the level of D-HPG was observed after 10 hr, and the final product concentration was about 50 m*M*. These results seem to be due to the fact that the activity of *N*-carbamoylase was lowered and inhibition of *N*-carbamoylase by the produced ammonia inside the *N*-carbamoylase-expressing cells became more serious with increasing pH. Figure 5C shows the production profile of D-HPG at pH 8.0. Initial production rate of D-HPG was as low

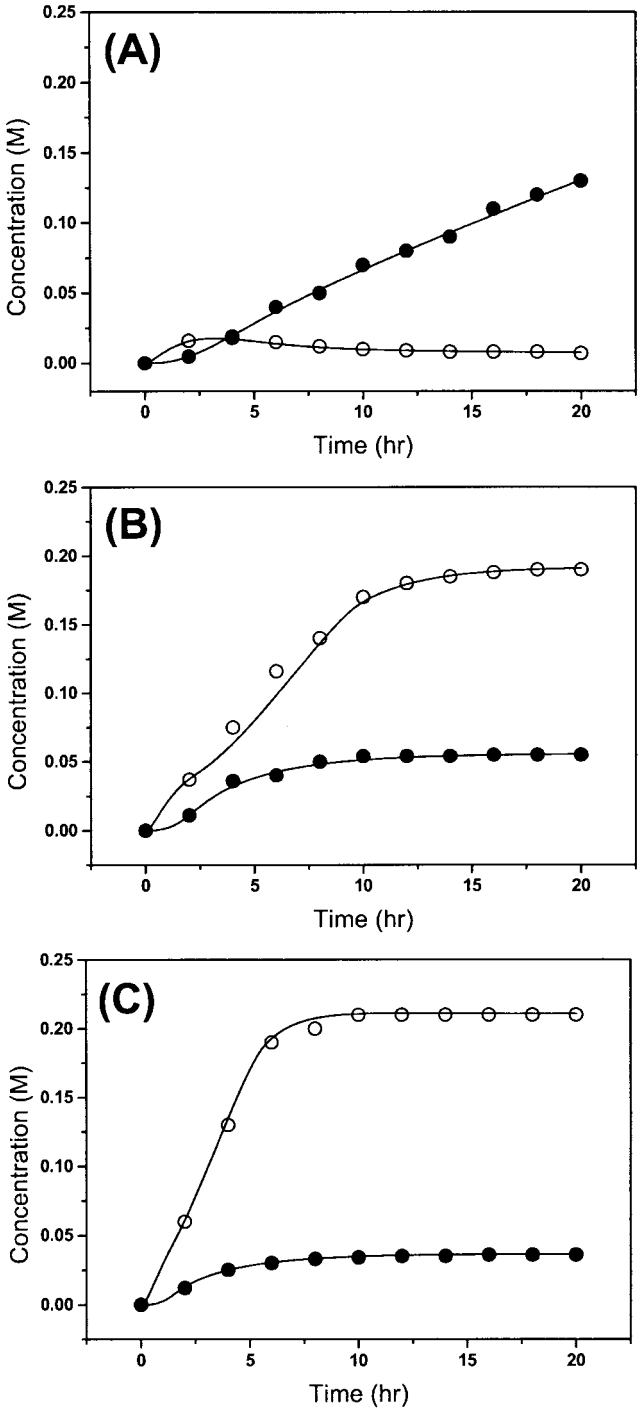

Figure 5. Reaction profiles using whole cells with separately expressed enzymes at different pH values: (A) 7.0; (B) 7.5; and (C) 8.0. Initial substrate concentration was 50 g/L (238 m*M*). The activities of D-hydantoinase and *N*-carbamoylase in the reaction mixture were the same as 50 u\units/g-HPH. Solid lines and symbols represent the simulated results and experimental data, respectively. Symbols: NC-D-HPG (○) and D-HPG (●).

as 2.3 m*M*/h and accumulation of the intermediate reached about 200 m*M* in 6 h. As mentioned above, the *N*-carbamoylase activity is relatively low at alkaline condition, and consumption rate of the intermediate by *N*-carbamoylase might be much lower than the production rate of the intermediate by D-hydantoinase, resulting in accumulation of the intermediate at high level. Consequently, the final product was maintained at 36 m*M* even for a prolonged reaction time.

Production profiles of D-HPG and intermediate were simulated and compared with the experimental data by increasing the activity of *N*-carbamoylase to D-hydantoinase at different pH values. The activity of D-hydantoinase was fixed at 50 units/g-HPH in the reaction mixture. Symbols represent the experimental data when the activity of *N*-carbamoylase was the same as the D-hydantoinase, and good agreements were observed with simulation results. At pH 7.0, accumulation of the intermediate decreases as the loading of *N*-carbamoylase increases in the reaction mixture as expected (Fig. 6A). When the activity of *N*-carbamoylase is 20 Units/g-HPH in the reaction solution, the intermediate level was predicted to be 25 m*M*. As the the *N*-carbamoylase activity increases to 150 units/g-HPH, the intermediate reaches about 10 m*M* and then gradually reduces to almost zero. As for the final product D-HPG, it increases linearly with reaction time and its production rate is almost the same regardless of the loading of *N*-carbamoylase, even though slight enhancement in the initial production rate of D-HPG is predicted (Fig. 6B). This result implies that the intermediate concentration inside the *N*-carbamoylase expressing cells is maintained at low level due to low transfer rate, leading to almost the first-order reaction kinetics.

When the pH of the reaction mixture is 7.5, the intermediate level remains high as a whole, even though the intermediate decreases with increasing loading of *N*-carbamoylase (Fig. 6C). Typically, accumulation of the intermediate is as high as 212 m*M* when the activity of *N*-carbamoylase is 20 units/g-HPH in the reaction mixture. Increment in the production rate of D-HPG with increasing loading of *N*-carbamoylase is more significant than at pH 7.0, but the level of the final product is much lower (Fig. 6D). These seem to be mainly caused by the fact that the *N*-carbamoylase activity decreases with increasing pH, but the activity of D-hydantoinase increases.

At pH 8.0, accumulation of the intermediate becomes more serious, reaching up to 232 m*M* in 8 hr when the loading of *N*-carbamoylase is 20 units/g-HPH in the reaction mixture (Fig. 6E). Increase in the loading of *N*-carbamoylase does not alleviate the accumulation of intermediate. The production rate of D-HPG increases as loading of *N*-carbamoylase increases, but the final product level at the corresponding activity of *N*-carbamoylase is much lower than at pH 7.5 (Fig. 6F). This result evidently comes from the unbalance between the production and conversion rates of the intermediate by the first and second-step enzymes. In other words, the activity of D-hydantoinase is much higher than *N*-carbamoylase at pH 8.0, and consequently the intermediate level becomes higher since consumption rate of the intermediate by

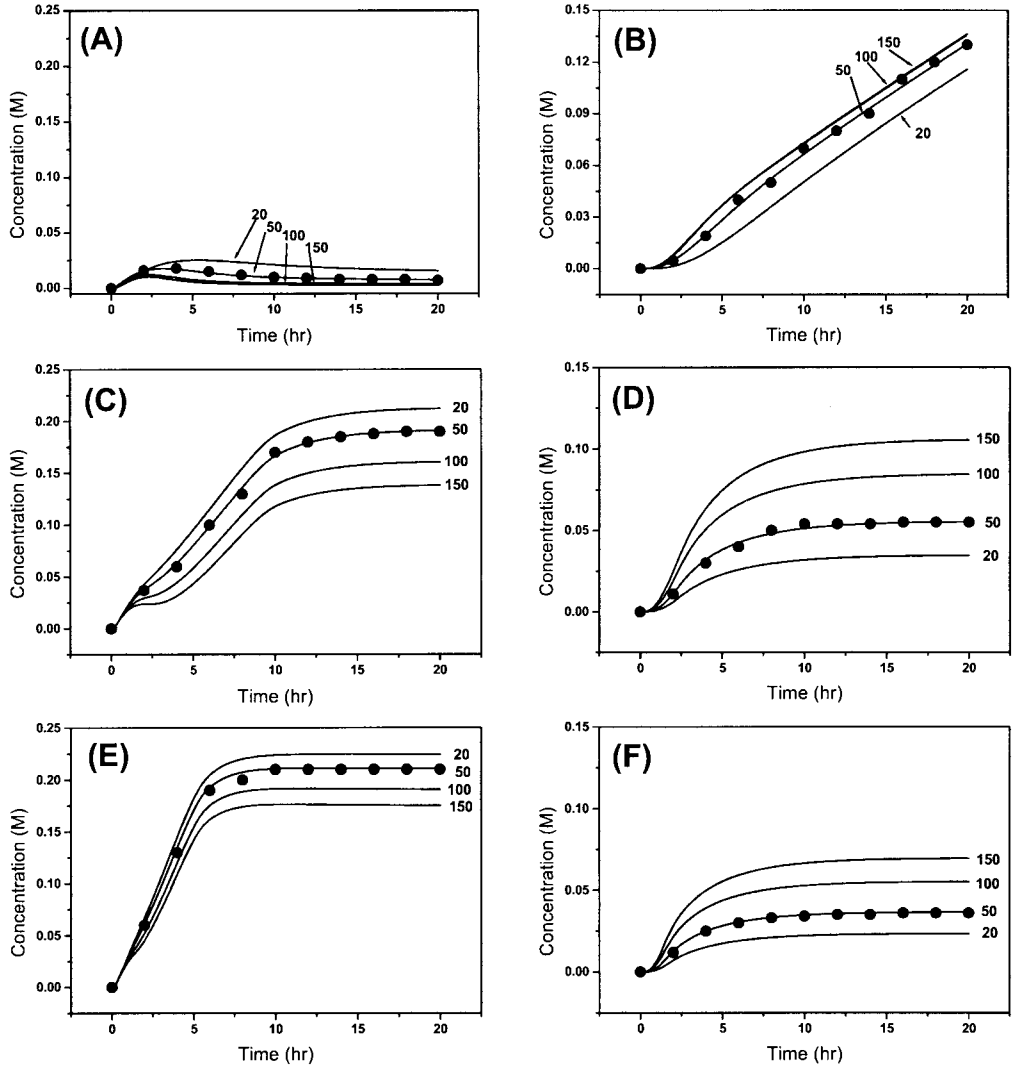

Figure 6. Effect of enzyme concentration on the production of NC-D-HPG and D-HPG at various pH values: NC-D-HPG at pH 7.0 (A), pH 7.5 (C), pH 8.0 (E) and D-HPG at pH 7.0 (B), pH 7.5 (D), pH 8.0 (F). The activity of D-hydantoinase in the reaction mixture was fixed at 50 Units/g-HPH. The denoted values indicate the *N*-carbamoylase activity in the reaction system. Solid lines and symbols represent the simulated results and experimental data, respectively.

N-carbamoylase is much lower than the production rate by D-hydantoinase. Inhibition of *N*-carbamoylase by ammonia at alkaline pH is also attributable to decrease in the production rate of the final product.

From the above results, it is evident that the mathematical models well describes the reaction system using whole cells with separately expressed D-hydantoinase and *N*-carbamoylase in the consecutive reaction. As the activity optima of the two enzymes are different with pH, the production rate of final product is largely affected by the pH of the reaction mixture.

Prediction of the Optimal Ratio Between D-Hydantoinase and *N*-Carbamoylase

To predict the optimal ratio between D-hydantoinase and *N*-carbamoylase in the reaction system with separately expressed enzymes, profiles of the final product were simulated at different pH values as a function of the ratio between the two enzymes (Fig. 7). At pH 7.0, the product concentration increases linearly with the ratio up to about 2.0 as expected, and then reaches a plateau. No further increase in the product concentration is predicted even for the ratio above 2.0, and this seems to be mainly due to the fact that the levels of D-*p*-HPH both within the cells and in the aqueous solution remain low due to a limited racemization rate of L-*p*-HPH at pH 7.0. As the pH increases, the product yield is significantly lowered, and this might be caused by the reduced activity of the second enzyme *N*-carbamoylase. Inhibition of *N*-carbamoylase becomes more serious with increasing pH, which also leads to lower product yield at alkaline condition compared to at pH 7.0. From the simulation results, the optimal ratio of *N*-carbam-

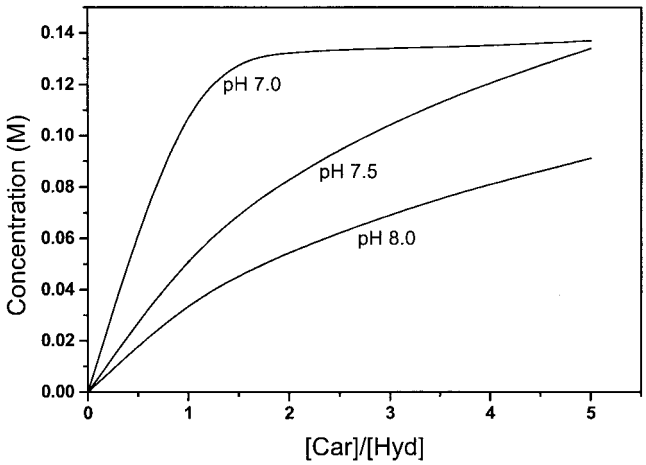

Figure 7. Effect of the activity ratio of *N*-carbamoylase to D-hydantoinase on the production of D-HPG at different pH values. Initial substrate concentration was 50 g/L. The activity of D-hydantoinase in the reaction mixture is 50 units/g-HPH. Car/Hyd represents the activity ratio between *N*-carbamoylase and D-hydantoinase. The activity of each enzyme was determined under standard assay condition.

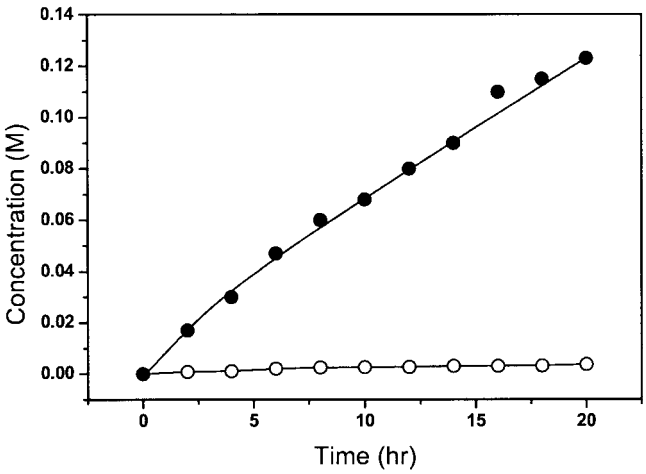

Figure 8. Production profiles of NC-D-HPG and D-HPG using whole cells with co-expressed enzymes at pH 7.0. Initial substrate concentration was 50 g/L, and the activities of D-hydantoinase and *N*-carbamoylase were 50 and 60 units/g-HPH, respectively. Solid lines and symbols represent the simulated results and experimental data, respectively. Symbols: NC-D-HPG (○) and D-HPG (●).

oylase to D-hydantoinase is predicted to be about 2.0, and the reaction at pH 7.0 results in highest product yield in the reaction system using whole cells with separately expressed enzymes.

Simulation of the Reaction System with Co-Expressed Enzymes

Based on the schematic diagram shown in Figure 2B, the reaction system using whole cells with co-expressed D-hydantoinase and *N*-carbamoylase was simulated at pH 7.0, and compared with experimental data. When the recombinant *E. coli* XL1 Blue/pHCAR101 expressing the two enzymes was assayed under standard condition, the ratio of activities between D-hydantoinase and *N*-carbamoylase per gram cells was determined to be about 1:1.2. As shown in Figure 8, the simulated production profiles of the intermediate and final product were well coincident with experimental results obtained at the D-hydantoinase activity of 50 units/g-HPH, which indicates that the kinetic model well describes the behavior of the reaction system using co-expressed enzymes. Production profile of the final product was similar to that in the reaction system using separately expressed enzymes. However, a much lower level of intermediate accumulated in the reaction mixture, and level of the product was higher than the separately expressed enzyme system. Linear increase in the final product implies that the reaction rate of the second enzyme *N*-carbamoylase follows the first-order kinetics due to low concentration of the intermediate inside the cells. As an advantage of the co-expressed enzyme system, the intermediate produced by the first enzyme D-hydantoinase is directly available for the secon D-step enzyme and readily converted to the final product, resulting in almost a zero level of intermediate in the reaction mixture.

The reaction performance was predicted in terms of the product yield and intermediate accumulation when the loading of whole cells co-expressing the two enzymes is increased in the reaction mixture (Fig. 9). As the loading of whole cells increases, the production rate of D-HPG is also enhanced, leading to higher product yield (Fig. 9A). The concentration of the final product approaches up to 184.9 m*M* when the activities of D-hydantoinase and *N*-carbamoylase are 150 and 180 Units/g-HPH, respectively. However, even though the loading of whole cells is increased as much as 3 times in the reaction mixture (i.e., 450 and 540 units/g-HPH for D-hydantoinase and *N*-carbamoylase, respectively), the product concentration is slightly increased. This result suggests that low racemization rate of the substrate at pH 7.0 limits the overall reaction of the co-expressed enzyme system.

To determine the optimal loading of enzyme in the reaction mixture, we simulated the effect of enzyme loading on the product yield at pH 7.0. The concentration of the final product was plotted as a function of the total activity of D-hydantoinase when the ratio of D-hydantoinase and *N*-carbamoylase is fixed at 1:1.2 (Fig. 9B). The concentration of the final product increases with increasing enzyme loading as expected. The enzyme loading above 200 Units/g-HPH of D-hydantoinase is shown not to be effective for the improvement of product yield. Based on the result, the optimal loadings of D-hydantoinase and *N*-carbamoylase are estimated to be about 200 and 240 units/g-HPH, respectively.

When the two enzymes are expressed in a single host, it is difficult to control precisely the expression level of

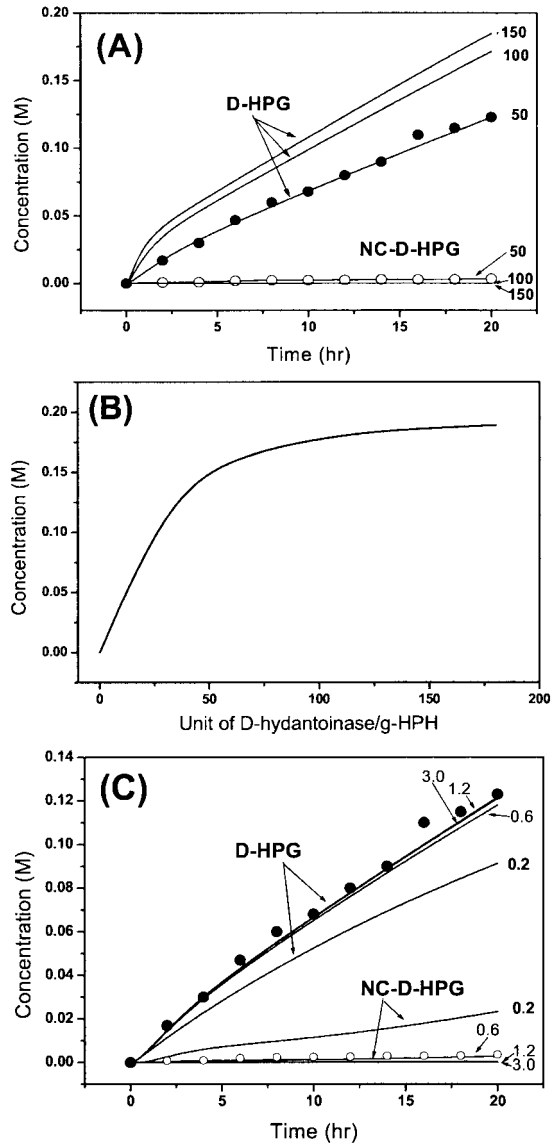

Figure 9. (A) Effect of enzyme concentration on the production of D-HPG in the co-expressed enzyme system. Initial substrate concentration was 50 g/L. The activities of D-hydantoinase were 50, 100, or 150 units/g-HPH, and the corresponding *N*-carbamoylase activities were 60, 120, and 180 units/g-HPH in the whole cells. Symbols: NC-D-HPG (○) and D-HPG (●). (B) Predicted product yield as a function of D-hydantoinase activity in the reaction mixture. The activity ratio of *N*-carbamoylase to D-hydantoinase within the whole cells was fixed at 1.2 on the basis of specific activity. (C) Effect of the activity ratio of *N*-carbamoylase to D-hydantoinase within the whole cells. Symbols indicate the experimental results obtained at the activity ratio of 1.2.

each enzyme and resultantly the activity ratio between the two enzymes in the reaction system. The production profiles were predicted at various activity ratios of *N*-carbamoylase to D-hydantoinase. As shown in Figure 9C, no significant effect is observed when the activity ratio is higher than 0.6. However, when the ratio is below 0.2, production of the final product is seriously reduced, and the intermediate accumulates at high level. Symbols represent experimental data obtained at the ratio of 1.2, and showed a good agreement with the simulation results.

Sensitivity Analysis

In order to evaluate the validity of the kinetic parameters and to investigate the effect of each parameter on the kinetics of the reaction system using whole cells with separately or co-expressed enzymes, the sensitivity for each parameter was typically examined for the reaction system using whole cells with co-expressed enzymes.

Effect of racemization coefficient on the production profiles of D-HPG at pH 7.0 is predicted in Figure 10A. Symbols represent the experimental results, and the simulation using the racemization coefficient of 3.2×10^{-5} cm/s gives a good agreement with experimental ones. The racemization coefficient ranging from 5.0×10^{-6} cm/s to 9.6×10^{-5} cm/s leads to a relatively large variation in the production profile. With the racemization coefficient of 3.2×10^{-5} cm/s, the concentration of D-HPG reaches 123 m*M* in 20 h. When the racemization coefficient is reduced to 1.0×10^{-5} cm/s, the final product concentration decreases to 73.3 m*M*. Increase of the coefficient to 9.4×10^{-5} cm/s results in the final product concentration of 196 m*M*. From these results, it is plausible that racemization rate of the substrate might limit the overall process in the reaction system. In this regard, use of microbial racemase at neutral or acidic pH is expected to improve the production rate of the final product.

The starting substrate, *p*-HPH, has a low solubility of 40 m*M* (7.6 g/L) in aqueous solution at 45°C, which might be one of the limiting factors in the reaction system. The influence of the substrate solubility on the profiles of the product formation was examined when the initial substrate concentration is fixed at 50 g/L. As shown in Figure 10B, the production of D-HPG significantly increases with increasing solubility, implying that solubility of the starting substrate can significantly affect the production rate of D-HPG. Simulation result using the solubility of 40 m*M* was well coincident with experimental one.

The effect of maximum permeability of the substrate and intermediate across the cell membrane on the production of D-HPG was analyzed. In this work, maximum permeabilities of substrate and intermediate were assumed to be the same and estimated to be about 3.5×10^{-6} cm/s under the reaction conditions when whole cells were used (Lee et al., 1999). As mentioned for the reaction system using separately expressed enzymes, the production rate was predicted to be significantly affected by the transfer of the intermediate into the cells expressing the second-step enzyme, *N*-carbamoylase. As can be seen in Figure

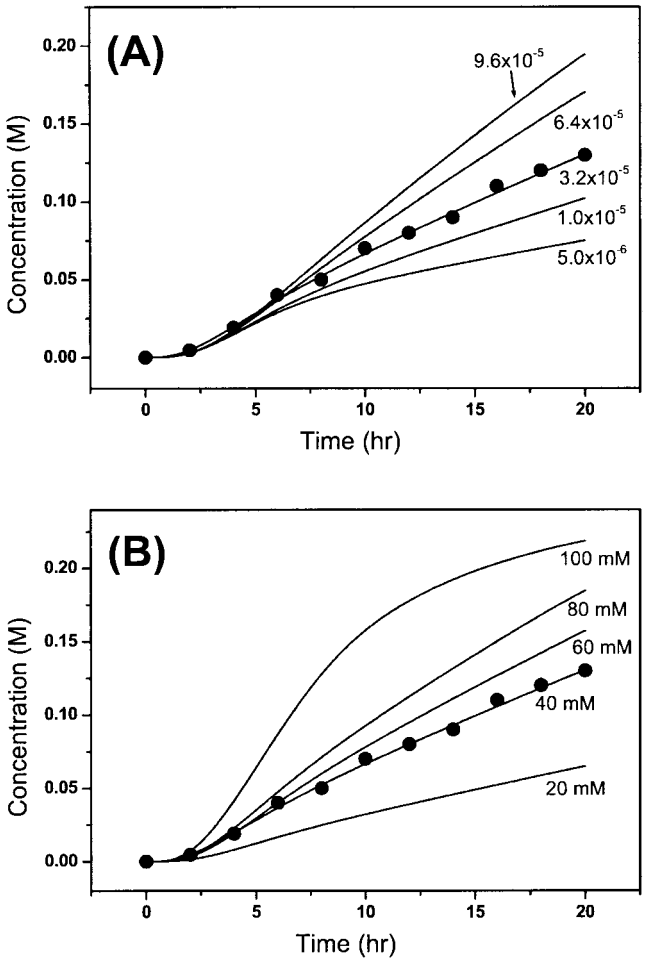

Figure 10. Effect of the racemization rate constant (A) and solubility (B) of the substrate on the production of D-HPG at pH 7.0. The activities of D-hydantoinase and *N*-carbamoylase in the reaction mixture were 50 and 60 units/g-HPH, respectively. Solid lines and symbols represent the simulated results and experimental data, respectively.

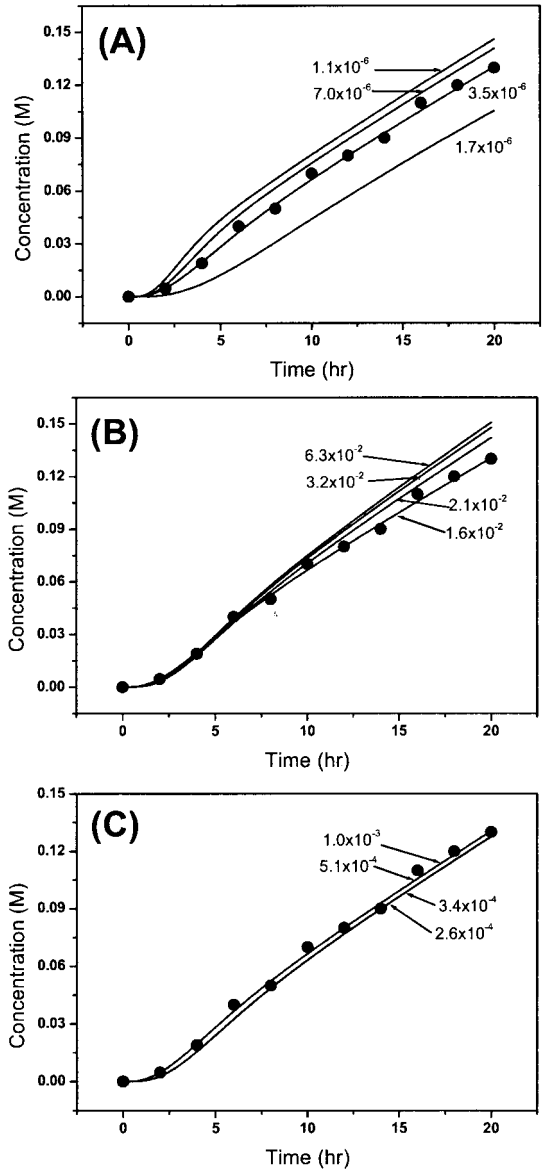

Figure 11. Effects of permeability of NC-D-HPG (A) and k_m values of D-hydantoinase (B) *N*-carbamoylase (C) on the production of the final product. The activities of D-hydantoinase and *N*-carbamoylase in the reaction mixture were 50 and 60 units/g-HPH, respectively. Solid lines and symbols represent the simulated results and experimental data, respectively.

11A, the concentration of the final product is increased with increasing permeability, but its production rate remains almost constant. The concentration of D-HPG reaches 149.2 m*M* in 20 h at the maximum permeability of 1.1×10^{-5} cm/s. When the permeability is increased three times, an increase in the final product is marginal, which implies that the effect of permeability on the production of the final product is not so significant compared to racemization rate or solubility of the substrate as for the reaction system using separately expressed enzymes.

In contrast to chemical catalysis, the catalytic property of enzyme is an important factor in the enzyme reaction. We investigated the effect of the Michaelis-Menten constant, k_m, on the product yield. As shown in Figure 11B, the production rate of D-HPG slightly increases even though the k_m value of D-hydantoinase is reduced as much as four times, indicating that the production rate of D-HPG is marginally influenced by the affinity of D-hydantoinase for the starting substrate. Simulation result with the k_m value of 6.3×10^{-2} mole/L exhibited a good agreement with experimental one. The similar results were observed in the case of *N*-carbamoylase. No significant change in the production rate and product yield is resulted from the increased affinity of *N*-carbamoylase (Fig. 11C). From these results, it follows that the production rate of the final product in the co-expressed enzyme system might be mainly affected by the physical factors including the solubility and racemization rate of substrate than catalytic affinity of enzymes.

The kinetic model developed here well described the reaction system using whole cells with separately or co-expressed D-hydantoinase and *N*-carbamoylase for the production of optically active D-amino acids. The present model might find applications to the optimization and development of the reaction system using two sequential enzymes.

NOMENCLATURE

a_P	specific surface area of substrate particles (cm^{-1})
ρ_s	density of substrate (mole/L)
A_{car}	suface area of the *N*-carbamoylase-expressing cells (cm^2)
A_{co}	suface area of the co-expressing cells (cm^2)
A_{hyd}	surface area of D-hydantoinase producing cells (cm^2)
E_{car}	concentration of *N*-carbamoylase inside cells (mole/L)
E_{hyd}	concentration of D-hydantoinase inside the cells (mole/L)
h	permeability of each compound (cm/sec)
h_0	initial permeability (cm/sec)
h_M	permeability of intermediate (cm/sec)
h_{max}	maximum permeability of each compound (cm/sec)
h_P	permeability of product across the cell membrane (cm/sec)
h_S	permeability of substrate across the cell membrane (cm/sec)
I_i	concentration of ammonia inside co-expressing cells (mole/L)
I_{ic}	concentration of ammonia inside *N*-carbamoylase-expressing cells (mole/L)
k_{cc}	catalytic constant of *N*-carbamoylase for intermediate (sec^{-1})
k_{ch}	catalytic constant of enzyme for the D-form substrate (sec^{-1})
k_{dc}	deactivation constant of *N*-carbamoylase at the defined condition (sec^{-1})
k_{dh}	deactivation constant of D-hydantoinase at the specified conditions (sec^{-1})
k_i	inhibition constant of ammonia (mole/L)
k_{mc}	Michaelis-Menten constant of *N*-carbamoylase for intermediate (mole/L)
k_{mh}	Michaelis-Menten constant of D-hydantoinase for the D-form substrate (mole/L)
k_R	racemization constant (sec^{-1})
k_s	mass transfer coefficient (cm/sec)
M_a	concentration of intermediate(mole/L)
M_i	concentration of NC-D-HPG inside the co-expressing cells (mole/L)
M_{ic}	concentration of NC-D-HPG inside the *N*-carbamoylase expressing cells (mole/L)
M_{ih}	concentration of intermediate, NC-D-HPG, in the D-hydantoinase-producing cells
N_P	the number of substrate particles in the aqueous solution (cm^{-3})
P_a	concentration of product in the aqueous solution (mole/L)
P_i	concentration of D-HPG inside co-expressing cells (mole/L)
P_{ic}	concentration of product, D-HPG, inside *N*-carbamoylase expressing cells (mole/L)
P_m	time required to reach the half of maximum permeability (sec)
R	radius of substrate particle (cm)
S^*	saturated concentration of *p*-HPH in water (mole/L)
S	concentration of *p*-HPH in the aqueous solution (mole/L)
S_{Da}	concentration of D-*p*-HPH in the aqueous solution (mole/L)
S_{Di}	concentration of D-form susbtrate inside cells (mole/L)
S_{La}	concentration of L-*p*-HPH in the aqueous solution (mole/L)
S_{Li}	concentration of L-form substrate inside cells (mole/L)
t	time (sec)
V_a	volume of aqueous solution (cm^3)
V_{car}	volume of the *N*-carbamoylase-expressing cells (cm^3)
V_{co}	volume of the co-expressing cells (cm^3)
V_{hyd}	volume of cells containing D-hydantoinase (cm^3)

References

Abendroth J, Chatterjee S, Schomburg D. 2000. Purification of a D-hydantoinase using a laboratory-scale streamline phenyl column as the initial step. J Chromatogr B 737:187–194.

Chao Y, Juang T, Chern J, Lee C. 1999. Production of D-*p*-hydroxyphenylglycine by *N*-carbamoyl-D-amino acid amidohydrolase-overproducing *Escherichia coli* strain. Biotechnol Progr 15:603–607.

Constantinides A. 1980. Steroid transformation at high substrate concentration using immobilized *Corynebacterium* simplex cells. Biotech Bioeng 22:119–136.

Grifantini R, Galli G, Carpani G, Pratesi C, Frascotti G, Grandi G. 1998. Efficient conversion of 5-substituted hydantoins to D-α-amino acids using recombinant *Escherichia coli* strains. Microbiology 144:947–954.

Ishikawa T, Watabe K, Mukohara Y, Nakamura H. 1997. Mechanism of stereospecific conversion of DL-5-substituted hydantoins to the corresponding L-amino acids by *Pseudomonas* sp. strain NS671. Biosci Biotechnol Biochem 61:185–187.

Jadhav SV, Pangarkar VG. 1991. Particle-liquid mass transfer in mechanically agitated contactor. Ind Eng Chem Res 30:2496–2503

Johnson ML, Faunt LM. 1992. Parameter estimation by least-squares methods. In: Brand L, Johnson ML, editors. Methods in enzymology, vol. 210. San Diego: Academic Press, Inc. p 1–36.

Keil O, Schneider M, Rasor J. 1995. New hydantoinase from thermophilic microorganisms synthesis of enantiomerically pure D-amino acids. Tetrahedron-Asymmetr 6:1257–1260.

Kim GJ, Kim HS. 1994. Adsorptive Removal of Inhibitory by-Product in the enzymatic production of optically active D-*p*-hydroxyphenylglycine from 5-substituted hydantoin. Biotechnol Lett 16:17–22.

Lee DC, Kim GJ, Cha YK, Lee CY, Kim HS. 1997. Mass production of thermostable D-hydantoinase by batch culture of recombinant *Escherichia co*li with a constitutive expression system. Biotechnol Bioeng 56:449–455.

Lee DC, Kim HS. 1998. Optimization of a heterogeneous reaction system for the production of optically active D-amino acids using thermostable D-hydantoinase. Biotechnol Bioeng 60:729–738.

Lee SG, Lee DC, Hong SP, Sung MH, Kim HS. 1995. Thermostable D-hydantoinase from thermophilic *Bacillus stearothermophilus* SD1: Characteristics of purified enzyme. Appl Microbiol Biotechnol 43:270–276.

Lee DC, Lee SG, Hong SP, Sung MH, Kim HS. 1996. Cloning and over-expression of thermostable D-hydantoinase from thermophile in *E. coli* and its application to the synthesis of optically active D-amino acids. Ann NY Acad Sci 799:401–405.

Lee DC, Park JH, Kim GJ, Kim HS. 1999. Modeling, simulation, and kinetic analysis of a heterogeneous reaction system for the enzymatic conversion of poorly soluble substrate. Biotechnol Bioeng 64:272–283.

Markus B, Peter W, Irving JD. 1999. Modeling of enzymatic reactions in vesicles: The case of α-chymotrypsin. Biotechnol Bioeng 62:36–43.

Ogawa J, Chung M, Hida S, Yamada H, Shimizu S. 1994. Thermostable *N*-carbomyl-D-amino acid amidohydrolase: screening, purification, and characterization. J Biotechnol 38:11–19.

Olivieri R, Fascetti E, Angelini L, Degen I. 1981. Microbial transformation of racemic hydantoins to D-amino acids. Biotechnol Bioeng 23:2173–2183.

Park JH, Kim GJ, Kim HS. 2000. Production of D-amino acid using whole cells of recombinant *Escherichia coli* with separately and co-expressed D-hydantoinase and *N*-carbamoylase. Biotechnol Prog 16:564–570.

Runser S, Chinski N, Ohleyer E. 1990. D-*p*-Hydaroxyphenylglycine production from D,L-5-*p*-hydroxyphenylhydantoin by *Agrobacterium* sp. Appl Microbiol Biotechnol 33:382–388.

Shugar GJ, Ballinger JT. 1996. Chemicall technicians' ready reference handbook, 4th ed. New York: McGraw-Hill, Inc. p 417.

Singleton P, Sainsbury D. 1987. Dictionary of microbiology and molecular biology, 2nd ed. New York: Wiley-Interscience.

Sudge S, Bastawde K, Gokhale D, Kalkote U, Ravindranathan T. 1998. Production of D-hydantoinase by halophilic *Pseudomonas* sp. NCIM 5109. Appl Microbiol Biotechnol 49:594–599.

Syldatk C, May O, Altenbuchner J, Mattes R, Siemann M. 1999. Microbial hydantoinase—Industrial enzymes from the origin of life? Appl Microbiol Biotechnol 51:293–309.

Tranchino L, Melle F. 1990. Modeling and control of the biocatalytic conversion of hydantoins to D-amino acid. Ann NY Acad Sci 589:553–568.

Wilms B, Wiese A, Syldatk C, Mattes R, Altenbuchner J. 2001. Development of an *Escherichia coli* whole cell biocatalyst for the production of L-amino acids. J Biotechnol 86:19–30.

Yamada H, Takahashi S, Kii Y, Kumagai H. 1978. Distribution of hydantoin hydrolyzing activity in microorganism. J Ferment Technol 56:484–491.